Available online at www.sciencedirect.com
ScienceDirect
Applied Geochemistry 22 (2007) 1293–1310
Applied Geochemistry
www.elsevier.com/locate/apgeochem

Cementation of kerogen-rich marls by alkaline fluids released during weathering of thermally metamorphosed marly sediments. Part I: Isotopic (C,O) study of the Khushaym Matruk natural analogue (central Jordan)

Serge Fourcade [a,*], Laurent Trotignon [b], Philippe Boulvais [a], Isabelle Techer [c], Marcel Elie [d], Didier Vandamme [e], Elias Salameh [f], Hani Khoury [f]

[a] *Géosciences Rennes UMR CNRS 6118, Université de Rennes 1, Campus de Beaulieu, 35042 Rennes Cedex, France*
[b] *CEA Cadarache DTN/SMTM/LMTE, Bât. 307, 13108 St Paul lez Durance, France*
[c] *Labo GIS/CEREGE, UMR CNRS 6635, Université d'Aix-Marseille 3, Parc Scientifique Georges Besse, 150 rue Georges Besse, 30035 Nîmes, Cedex 1, France*
[d] *UMR CNRS 7566-G2R, Université H. Poincaré, BP 239, 54501 Vandoeuvre-les-Nancy Cedex, France*
[e] *CEREGE, UMR CNRS 6635, Université d'Aix-Marseille 3, Technopôle du Petit Arbois, BP 80, 13545 Aix-En-Provence Cedex 4, France*
[f] *Department of Geology, University of Jordan, P.O. Box 17167, Amman 11942, Jordan*

Received 12 October 2005; accepted 14 February 2007
Editorial handling by M. Gascoyne
Available online 30 March 2007

Abstract

The Khushaym Matruk site in central Jordan may represent a natural analogue depicting the interaction of alkaline solutions with a clayey sedimentary formation or with clay-rich confining barriers at the interface with concrete structures in waste disposal sites. In this locality, past spontaneous combustion of organic matter in a clayey biomicritic formation produced a *ca.* 60 m-thick layer of cement-marble containing some of the high-temperature phases usually found in industrial cements (e.g., spurrite, brucite, and Ca-aluminate). A vertical cross-section of the underlying sediments was used in order to study the interaction between cement-marbles and neighbouring clayey limestones under weathering conditions. A thermodynamic approach of the alteration parageneses (calcite–jennite–afwillite–brucite and CSH phases) in the cement-marbles constrains the interacting solutions to have had pH-values between 10.5 and 12. Over 3 m, the sediments located beneath the metamorphic unit were compacted and underwent carbonation. They display large C and O isotopic variations with respect to "pristine" sediments from the bottom of the section. Low δ^{13}C-values down to $-31.4‰$/PDB show the contribution of CO_2 derived from the oxidization of organic matter and from the atmosphere to the intense carbonation process affecting that particular sedimentary level. The size of the C isotopic anomalies, their geometrical extent and their coincidence with the variations of other markers like the Zn content, the structure of organic matter, the mineralogical composition, all argue that the carbonation process was induced by the percolation of high pH solutions which derived from the alteration of cement-marbles. The temperature of the carbonation process remains conjectural and some post-formation O isotopic reequilibration likely affected the newly-formed carbonate. Carbonation induced a considerable

* Corresponding author. Tel.: +33 2 99 286179; fax: +33 2 99 28 67 80.
E-mail address: fourcade@univ-rennes1.fr (S. Fourcade).

0883-2927/$ - see front matter
doi:10.1016/j.apgeochem.2007.02.012

porosity reduction, both in fractures and matrixes. The Khushaym Matruk site may have some bearing to the early life of a repository site, when water saturation of the geological formations hosting the concrete structures is incomplete, enabling simultaneous diffusion of alkaline waters and gaseous CO_2 in the near field.

1. Introduction

In France, the concept of a geological disposal for high-activity, long-period nuclear wastes requires the use of concrete and cement-bearing materials as building structures or as waste containment packages, in conjunction with clayey barriers (e.g., compacted bentonite as an engineered barrier and/or argillite-type rocks as a geological barrier). Previous work has demonstrated that hydrolysis of cementitious phases produces hyper-alkaline pore fluids with pH ranging from 10 to 13.5 (e.g., Adenot and Buil, 1992, and references therein). Migration of such chemically aggressive fluids could alter the confining properties of the clayey barriers and therefore, numerous studies have been carried out on the behavior of clay minerals and argillaceous rocks in the presence of hyper-alkaline solutions (e.g., Braney et al., 1993; Eberl et al., 1993; Bauer and Berger, 1998; Adler et al., 1999; Bauer and Velde, 1999; Bateman et al., 1999; Ramirez et al., 2002; Herbert et al., 2002; Savage et al., 2002; Soler, 2003; Mosser-Rück and Cathelineau, 2004). From these studies, a number of mineralogical effects have been found. Sodium may be partly replaced by K in smectite, leading to the transformation of smectite into illite, if K is available in the system. K-feldspar and quartz are dissolved and secondary phases, most frequently clays, zeolites and Ca silicate hydrates (CSH) may crystallize. Besides the knowledge of mineral/solutions reaction paths, the spatial extent of potential damage induced by the intrusion of an alkaline plume into the confining clayey material (distance, diffusive or advective alteration patterns) is also of great importance as it concerns the safety assessment of a deep disposal. Modeling approaches argue that mineralogical disturbances due to high-pH solutions are observed on a limited distance away from the cementitious source, which may be explained by the buffering capacity of smectites in such conditions. Gaucher et al. (2004) argued that the extent of the perturbations is proportional to the square root of the diffusion time and to the diffusion coefficient. In compacted bentonite, the calculated perturbation reaches a few decimetres to a few metres for reasonable diffusion coefficients after 100 ka, one of the characteristic timescales for storage viability. According to De Windt et al. (2004), the pore water chemistry in a clayey rock formation (argillite) could be affected over distances up to 10 m.

In some rare natural systems, the mineral phases known to result from interaction between high-pH solutions and various clay minerals are identified. These systems occur where clayey limestones rich in organic matter and submitted to combustion metamorphism are exposed to weathering, for example, the ''Mottled Zone'' in Israel (Kolodny and Gross, 1974), the sites of Maqarin (Khoury et al., 1985, 1992; Alexander et al., 1992; Clark et al., 1993; Alexander and Smellie, 1998) and of Khushaym Matruk in Jordan (Techer et al., 2004, 2006). Such sites may constitute natural analogues of concrete/clay matrix interfaces in repository sites where the extent and mechanism of migration may be assessed for various elemental species over geological timescales. In the Maqarin site, the production and flow of current alkaline solutions have been investigated. The Khushaym Matruk site (KHM), where the alkaline flow system is presently inactive, offers an additional opportunity to unravel the impact of such alkaline fluids within a clay-bearing rock because it displays an horizontal transition zone between metamorphic rocks and clay-bearing sediments. It has been investigated in terms of mineralogy and Sr isotopic ratios by Rassineux (2001) and Techer et al. (2004, 2006). These authors showed that mineral variations and Sr isotopic compositions in the clay-bearing sediments are compatible with alteration by alkaline solutions produced by weathering of cement-marbles. The aim of the present study in the KHM site is (i) to specify the high pH of the fluid involved, (ii) to quantify the geometrical extent of the percolation of the alkaline plume, (iii) to constrain the solution – rock interaction mechanism, and (iv) to assess the relevance of the site as being an analogue of a clay–concrete interface in a repository site. For that purpose, for a series of sediments in contact with natural ''cement marbles'', the C and O isotopic ratios of the carbonate components (global analysis and in situ micro-analysis), the C isotopic ratio and

maturation state of organic matter and the rocks magnetic susceptibility, were measured. The two last aspects are presented in a companion paper (Elie et al., 2007).

2. Geological setting and sampling strategy

The Khushaym Matruk site is located in Central Jordan, at about 80 km SE of Amman in a desert area (Fig. 1) (Smellie, 1998; Techer et al., 2006). Exposed rocks are rather homogeneous and represented by grey clayey biomicritic limestones of the *Muwaqqar Formation* ranging in age from Maestrichtian to lower Paleocene. The rocks mostly contain carbonates (66–83%) and clays (10–15%) of illite-smectite type (smectite layers 80%) close to beidellite (Techer et al., 2004, 2006). Other minor components are detrital quartz, K-feldspar, apatite and mica. The amount of organic matter is considerable, around 4–7% (Elie et al., 2007).

In the studied site, the flat-lying clayey biomicrites are exposed over 10 m of vertical elevation at the bottom of a small hill. The upper part of the hill is made of a thick cement-marble unit (60 m) formed by high-temperature metamorphic recrystallization of the clayey limestones during spontaneous combustion of the organic matter. Beneath the metamorphic zone, over 2.5–3 m, the underlying clayey limestones (labelled A3 level, Fig. 2) were hardened but they do not contain any metamorphic mineral. For convenience, these rocks are qualified as "baked biomicrites" hereafter. Rocks of the A3 level are crosscut by numerous millimetre- to micrometre-thick white and green veinlets having a rather planar shape and mainly filled by carbonates and clays (Techer et al., 2004, 2006). Beneath the A3 level, the clayey limestones (A2 level) that are exposed over *ca.* 6 m of vertical elevation are crosscut by centimetre-thick veins filled with gypsum (Fig. 2). Presumed pristine sediments are found at the bottom of the pile (A1 level, Fig. 2). The upward evolutions summarized in Fig. 2 are (Rassineux, 2001; Rassineux et al., 2001; Techer et al., 2004, 2006): (1) the decrease of the illite-smectite mixed layers crystallinity, (2) the evolution of the clay chemical composition, (3) the decrease of smectite layers in the illite-smectite mixed-layer clays (from 80% to 60%), (4) the (re)crystallization of calcite and growth of zeolite and (5) the disappearance of detrital quartz and feldspar (absent in level A3). Travertine pods are observed mostly at the contact between the metamorphic unit and the A3 rock unit where many cavities are observed and at one other discrete level between the contact and the hilltop. Small-size travertine-rich crusts are locally found at the hilltop.

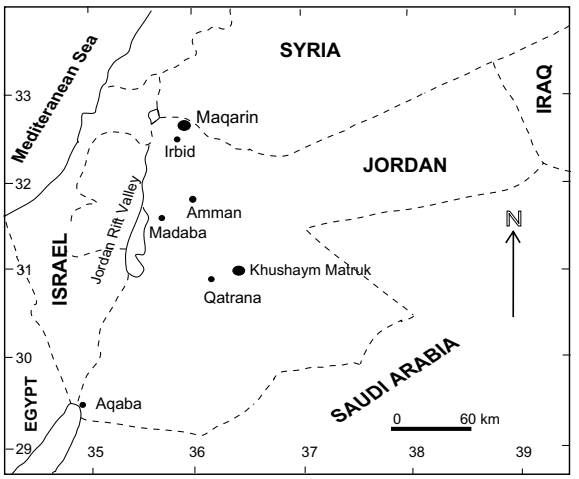

Fig. 1. Sketch location map of the Khushaym Matruk site in central Jordan. The Maqarin site, located in northern Jordan is also reported.

The KHM site may be seen as a natural example of a concrete/clayey matrix industrial interface only if it could be identified as a low-temperature interaction system with high pH hydrous fluids. Therefore, the sediments underlying the metamorphic cement-marble unit are the target of the study because they likely bear information on the impact of both the thermal event and the flow of alkaline solutions. Potential tracers sensitive to temperature or to fluid/rock interaction, – i.e. isotopic tracers (C, O), chemical tracers (e.g., Zn contents), magnetic susceptibility, maturation state of organic matter – were measured in the matrix of these transitional, baked biomicrites. Newly-formed carbonates, like veins and travertines, and far-seated biomicrites were also analysed as being reference members of the system, while the mineral characterization of a few cement-marbles was undertaken in order to evaluate the possible pH of the solutions released upon alteration. A trench was dug along the hillside with a depth of *ca.* 1 m in order to remove potentially-weathered surface rocks. Along that trench, the 10 m-thick sedimentary pile was sampled and each sample was carefully positioned with respect to the flat-lying interface with the overlying cement-marble unit (metre marks are counted positively downward, Fig. 2). A few cement-marbles were also picked up at the hilltop and a few about 20 m under it.

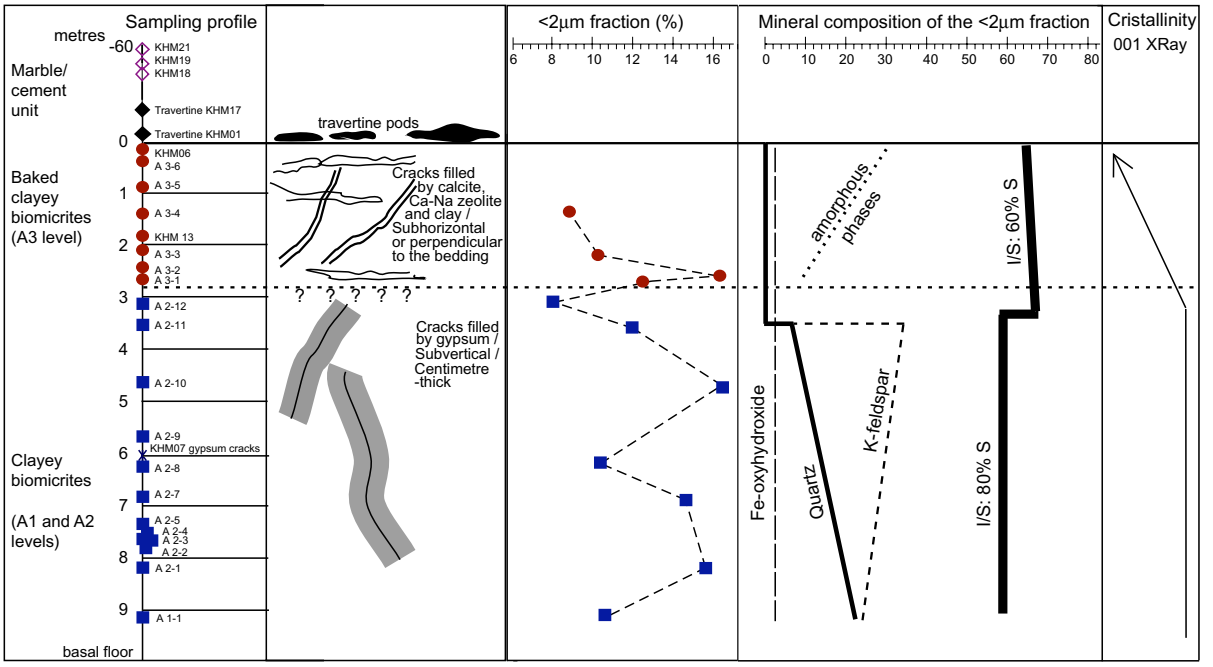

Fig. 2. Localization of the studied samples on a vertical profile (metre marks are counted positively downward) with some relevant information on the structural and mineralogical variations observed (after Rassineux, 2001).

3. Analytical techniques

3.1. Mineralogical characterization

The cement-marble unit was characterized in terms of its mineral composition by microscopic observations and X-ray diffraction measurements. A thin slab ($2 \times 4\ cm^2$) of a sample (BL2b, 20 m below the hilltop) was sawed in the rock mass in order to select a region with well-preserved fractures. This slab was then polished with water free diamond suspensions (9, 3 and 1 µm). The sample was observed under a binocular microscope and also using SEM/EDX investigations (Philips XL 30 ESEM and Oxford/Link EDX system, 20 kV, working distance 10 mm.) In addition, several XRD spectra were recorded on powdered fractions of the different parts of the sample (Brüker D8, Cu cathode): unaltered cement matrix, altered cement matrix and fracture infillings.

3.2. Stable isotopes

Carbon and O isotopic compositions were investigated both on whole rocks of the profile and on the carbonate material filling the fractures. The sample of baked biomicrite A3-6, located 0.5 m beneath the contact, was carefully investigated on a smaller scale. It displays an heterogeneous colour pattern (from dark grey to light grey) and also different carbonate-bearing veins. Early veins are generally parallel to the sediment layering and later oblique fractures cross-cut the previous ones (Fig. 3a). Chips corresponding to light and dark areas were extracted from that sample as well as the fracture infillings (Fig. 3b). The sample of baked biomicrite A3-6 was also studied by small-scale in situ analysis of C isotopic ratios (foraminifera, microveins, matrix, Fig. 3c). Attempts to obtain perfectly polished sections on biomicrite samples located deeper in the profile were unsuccessful because these rocks were too porous and friable.

Bulk rock samples correspond to a few cm^3 of powdered material. This amount was reduced to *ca.* 1/20th of a cm^3 for sub-samples A3-6. Fracture infillings were extracted by micro-drilling and scratching off. The carbonate fraction (1–10 mg) was reacted with 100% orthophosphoric acid at 25 °C (McCrea, 1950) using $\alpha(O)\ CO_2/CaCO_3$ (extraction) = 1.01025. Selected samples of biomicrites were enriched in their organic matter component (OM) by reaction with excess dilute HCl, then washed with distilled water, centrifuged and dried. After degassing, OM-enriched samples were reacted with purified CuO in sealed tubes of silica glass at 900 °C.

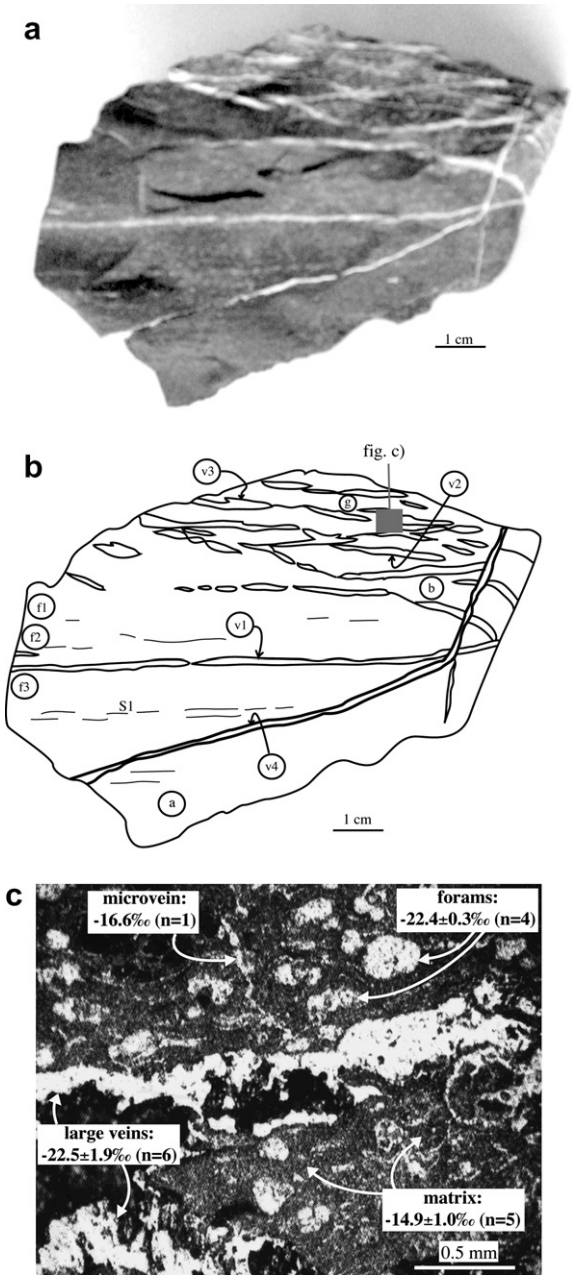

Fig. 3. (a) View of baked biomicrite sample A3-6 (metre mark 0.5 m) with (b) a sketch showing the location of analyzed matrix and vein sub-samples and (c) a microscopic view of the polished area studied using ion-microprobe with the corresponding C isotopic compositions ($\delta^{13}C$ vs. PDB). In (c), calcite appears as a light mineral while the dark material in the large vein is zeolite.

Isotopic analyses were carried out on CO_2 gas using a VG SIRA 10 mass spectrometer at Géosciences Rennes and expressed, using internal carbonate standards, the USGS 24 graphite and the NBS 19 reference material, with the conventional δ notation vs. SMOW (O) and PDB (C). The average uncertainties on C and O analyses are estimated to be $<0.1‰$ (C) and *ca.* $0.1‰$ (O). The carbonate content of bulk rocks was also measured during CO_2 extraction with a manometer.

In situ C analysis of calcite cements in the microscopic matrix of sample A3-6 was performed by secondary ion mass spectroscopy (SIMS) on the Caméca IMS1270 at CRPG, Nancy (France). Measurements were done on standard polished thin sections coated with Au by use of a 25 nA defocused primary ion beam of Cs^+ (impact energy of 10 keV), following the method of Rollion-Bard et al. (2003). Sub-circular ablation craters of 30 μm were produced by analysis. Mass resolution of 5000 was used for C isotopes analyses. Carbon isotopes were measured in multicollection mode using one off-axis Faraday cup (L′2) and the central electron multiplier. Typical ion intensities of 2.10^7 counts per sec (cps) were obtained on the ^{12}C, so that an internal 1σ error of $\pm0.1‰$ to $0.2‰$ was reached after a few minutes of counting. The average external reproducibility, as estimated from replicate measurements of carbonate standards, was $\pm0.4‰$. Instrumental mass fractionation was corrected considering the isotopic values of the calcite standards known by conventional analysis.

In addition, for the purpose of comparison, the C and O isotopic compositions of selected carbonate stalactites produced after concrete structures were also analysed. Sampling areas were carefully chosen so that anthropogenic (e.g., fuel combustion exhausts or respiration) or plant (photosynthesis, and respiration) contributions to the budget of local atmospheric CO_2 were minimal. Stalactites hanging on rural bridges over rivers and in other well-vented rural situations were found to be adequate for that purpose.

3.3. Porosity measurements

Porosity parameters (total connected porosity, average pore diameter) were measured in the University of Caen (France), using Hg injection, on 5 samples selected across the profile.

3.4. Analysis of Zn

Bulk samples of the rocks collected along the trench profile were ground in an agate mortar and then attacked using classical techniques (alkaline fusion, acid dissolution). Analysis of the solutes

was done with a Jobin-Yvon ICP-AES spectrometer. The relative error on Zn concentrations is estimated at 10%.

4. Results

4.1. Mineralogical characterization of the cement source term

The unaltered cement, far from the large fractures, shows a red-brown fine-grained matrix in which large translucent calcite crystals (from 5 μm to more than 50 μm in diameter), as well as red-black nodules (diameters from 50 μm to 300 μm) containing Fe oxides (hematite colour) are visible. A SEM BSE image of this unaltered matrix is presented in Fig. 4. Calcite sometimes occurs as round shaped grains inside another undetermined phase labelled Mineral "X" (undetermined calc-silicate-sulphate containing K). Spurrite ($Ca_5(SiO_4)_2CO_3$) is clearly identified and occurs as crystals ranging from 5 to 15 μm in diameter. Calcite and spurrite represent the two dominant minerals of this matrix. Mineral "X" appears as very bright rectangular patches around 50 μm long and 20 μm wide. This phase also contains minute $BaSO_4$ inclusions. Several other minor phases could be identified: a phosphate rich phase that could be identified as ellestadite, brownmillerite ($Ca_2(Al,Fe)_2O_5$), brucite ($Mg(OH)_2$), visible as very dark intergrain zones in Fig. 4, and an undetermined Ca aluminate occurring as grey fillings in Fig. 4.

Adjacent to the large fractures, the cement matrix is bleached (beige) on a width of 1–4 mm. The width of this zone seems to be roughly proportional to the width of the internal fracture. A sharp front showing some colour texture separates this altered matrix from the intact red-brown material. It corresponds to the dissolution front of spurrite, as can be seen by SEM. In the altered matrix where spurrite is no longer present, Ca–Si hydrated gels (CSH) are found instead, between the calcite crystals. Major fractures (~100 μm width) are filled with white, grey or yellowish products. Thin fractures (~10 μm in width) show white infillings. Fracture fillings consist mainly of jennite ($Ca_9H_2Si_6O_{18}$–$6H_2O$) and calcite, with inclusions of $Ba((1-x)SO_4, xCrO_4)$ crystals. Portlandite was not identified.

The XRD spectrum of the powdered material representing the unaltered matrix shows its strongest lines for calcite (05-0586) and spurrite (75-0620). Because these phases have a lot of diffraction

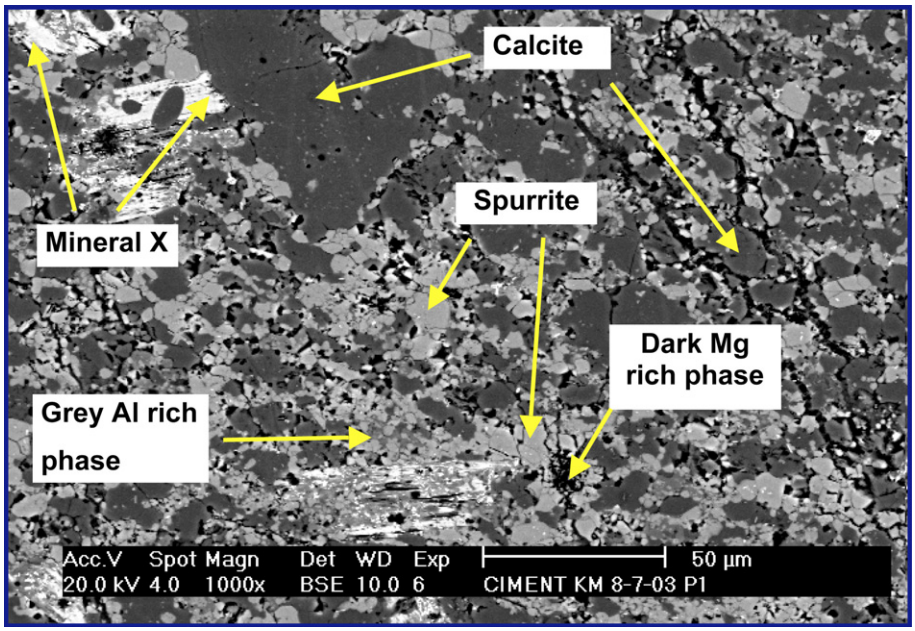

Fig. 4. Cement-marble sample (BL2b): BSE-SEM image showing major mineral phases of the cement on a polished crossed section. Calcite and spurrite are the two main mineral components of the unaltered rock. Dark Mg-rich phase: brucite-like compound, grey Al-rich phase: Ca aluminate, mineral X: undetermined Ca-silicate-sulphate containing K.

lines, it is difficult to attribute weak residual lines that are frequently overlapped or edged by strong calcite or spurrite peaks. However, the attribution of several lines to brucite (44-1482) is proposed, consistently with SEM observations. The XRD spectrum of the altered matrix differs mainly by the absence of the lines of spurrite. Lines of afwillite ($Ca_3Si_2O_4(OH)_6$) (weak) and jennite (medium) are identified. The XRD spectrum of powdered material collected from the inner fracture fillings revealed the presence of mainly calcite and jennite and, to a lesser extent, thaumasite and ettringite.

4.2. C and O isotopic compositions

Isotopic data are reported in Table 1 and Fig. 5.

4.2.1. Bulk compositions

Four main groups of C and O isotopic compositions are identified.

(1) The first group is close to the isotopic compositions of marine carbonates and corresponds to the matrix carbonate fraction of those clayey biomicrites which are located at the bottom of the hill (metre marks between 9.1 and 7.85): $\delta^{18}O = 28.1$ to 28.4‰ and $\delta^{13}C = -2.6$‰ to -4.4‰. Such "primitive" values correspond to marine carbonates which are only weakly modified by diagenesis. These values can be measured locally in rocks located higher in the profile (6.2 m and 5.8 m).

(2) The second group with low δ^{13}C-values around -15‰ corresponds to the carbonate fraction of cement-marbles (KHM 18, 19, 21). Oxygen isotopic compositions are also lower than those of the previous group with δ^{18}O-values ranging from 18.4‰ to 23.7‰. These compositions are close to those reported in cement-marbles of the Maqarin site, which formed by a similar combustion process at the expense of a more carbonate-rich lithology (Clark et al., 1993).

(3) The third group of isotopic compositions corresponds to the matrix carbonate fraction of the clayey biomicrites which are found in the upper part of the profile, between metre marks 0 and 6.9. This group is characterized upwards, by an increase of the carbonate content (Fig. 6a) and a decrease of δ^{13}C-values (Fig. 6b). It is worth noting that above metre mark 3, the δ^{18}O-values are lower than in "pristine" biomicrites and remain rather constant (20.6 to 22.6‰, Fig. 6c). The carbonate fraction of the gypsum-rich centimetre-thick cracks has similar isotopic ratios.

(4) The fourth group with low to very low δ^{13}C-values (from -15‰ to -31.5‰) corresponds to newly-formed carbonate from travertines and to vein carbonate found in the A3 level. In the veins, the O isotopic composition is, like in group (3), lower than the marine references. The lowest δ^{13}C-value is reached in vein KHM13 that also displays the lowest δ^{18}O-value (16.4‰). Travertines have somewhat higher δ^{18}O-values (23.6‰ and 24.5‰).

4.2.2. Organic matter

In contrast to matrix carbonate, the $^{13}C/^{12}C$ ratio of organic matter does not change significantly over the studied section (Fig. 6b), taking into account the possible pre-combustion (sedimentary) variability. Only a slight δ^{13}C increase (*ca.* 1 δ-unit) may exist in the A3 level.

4.2.3. Sub-samples and in situ analyses of A3-6 baked biomicrite

The newly-formed carbonate fraction from flat-lying veins has low δ^{13}C-values (-19.7‰ to -21.2‰) as similar veins from the neighbouring rocks in A3 level (Fig. 3, Table 1). Matrix carbonate does not show marine isotopic signatures but displays low δ^{13}C-values (-15.9‰ to -18.1‰) that are intermediate between those of the veins and those of the reference "pristine" biomicrites at the bottom of the profile. The δ^{13}C-values are related to the matrix local darkness and in turn, to its calcite content (Figs. 3a and 7). High resolution in situ analyses show: the highest $^{13}C/^{12}C$ ratios are found in the matrix ($\delta^{13}C = -14.9 \pm 1.0$‰) while newly-formed carbonates filling up foraminifera and fractures share comparable low δ^{13}C-values (-22.5 ± 1.0‰ and -22.4 ± 0.3‰, respectively). One noticeable exception to the general picture is the late carbonate vein V4 that cross-cuts the bedding at a high angle (Fig. 3a and b). This sample has a much lower δ^{13}C-value (-26.3‰, Table 1) compared to the rest of sample A3-6. All the carbonates analysed, regardless of their situation, possess rather constant δ^{18}O-values (20.2 to 22.2‰), comparable to those of the other samples from level A3.

Table 1
Isotopic compositions of carbonates and kerogen in the Khushaym Matruk clayey biomicrites and a few overlying cement-marbles

Sample	Metre mark	Type	wt% calcite	δ^{18}O cal	δ^{13}C cal	δ^{13}C OM
A 1-1	9.1	Clayey biomicrite	67	28.03	−2.56	−26.7
A 1-2	8.6	Clayey biomicrite				−26.8*
A 2-1	8.2	Clayey biomicrite	71	28.12	−3.87	−27.4*
A 2-2	8.1	Clayey biomicrite	68	28.36	−3.63	
A 2-3	8.0	Clayey biomicrite				−27.2*
A 2-4	7.95	Clayey biomicrite	71	28.41	−4.38	−27.5/−27.8*
A 2-5	7.85	Clayey biomicrite		28.09	−3.33	−27.7/−28.3*
A 2-7	6.9	Clayey biomicrite	70	27.71	−6.51	
A 2-8	6.25	Clayey biomicrite	60	27.60	−4.42	
A 2-8 ep	6.25	Edge of crack KHM 07	9	27.59	−4.92	
KHM 07	6.0	Crack gypsum+calcite infilling		24.95	−4.47	
KHM 08	6.0	Clayey biomicrite				−27.5*
A 2-9	5.8	Clayey biomicrite	71	27.28	−2.91	−26.6
A 2-10	4.7	Clayey biomicrite	77	24.19	−4.69	−27.0
A 2-11	3.6	Clayey biomicrite	75	25.54	−5.06	−26.5
A 2-12	3.05	Clayey biomicrite	68	22.33	−6.18	−26.9
A 3-1	2.7	Baked clayey biomicrite	77	21.23	−9.85	−26.4
A 3-1b	2.7	Baked clayey biomicrite	81	21.17	−11.44	
A 3-2	2.6	Baked clayey biomicrite	72	22.29	−9.38	−26.3*
A 3-2 (nodules)	2.6	Black nodules in baked clayey biomicrite	33	22.40	−5.99	
A 3-2 (vein)	2.6	Calcite vein	100	22.51	−10.21	
A 3-3	2.1	Baked clayey biomicrite				−25.4*
KHM 13 (matrix)	2.0	Baked clayey biomicrite	60	20.65	−16.88	−25.1*
KHM 13 (vein)	2.0	Calcite + gypsum vein	80	16.40	−31.36	
KHM 14	2.0	Baked clayey biomicrite				−25.5
KHM 15	2.0	Baked clayey biomicrite				−25.3*
A 3-4	1.4	Baked clayey biomicrite	74	22.08	−12.97	
A 3-4 (vein)	1.4	Calcite vein	100	22.20	−17.45	
A 3-5a	1.0	Dark brown baked clayey biomicrite		21.59	−17.29	−25.7
A 3-5b	1.0	Pale brown baked clayey biomicrite		22.28	−25.44	
A 3-5c	1.0	Calcite vein (parallel to cleavage)		21.70	−20.57	
A 3-5f	1.0	Calcite + zeolite-bearing crack	95	21.43	−22.06	
A 3-6a	0.5	Baked clayey biomicrite	70	20.66	−16.03	
A 3-6b	0.5	Foram-bearing baked clayey biomicrite	89	20.71	−18.07	
A 3-6f1	0.5	Baked clayey biomicrite	70	20.60	−16.50	
A 3-6f2	0.5	Baked clayey biomicrite	59	20.43	−15.93	
A 3-6f3	0.5	Baked clayey biomicrite	61	20.59	−16.02	
A 3-6g	0.5	Foram-bearing baked clayey biomicrite	70	20.83	−17.64	
A 3-6v1	0.5	Calcite vein (parallel to cleavage)	100	20.20	−19.69	
A 3-6v2	0.5	Calcite vein (parallel to cleavage)	100	22.15	−22.35	
A 3-6v3	0.5	Calcite vein (parallel to cleavage)	100	22.16	−21.24	
A 3-6v4	0.5	Calcite vein (oblique to cleavage)	100	21.19	−26.28	
KHM 06 (matrix)	0.25	Travertinous biomicrite	84	22.58	−28.70	−26.7
KHM 06 (belemnite)	0.25	Belemnite in baked clayey biomicrite	100	22.22	−28.80	
KHM 01c	0	Pink travertine	100	24.55	−20.14	
KHM 04	0	White-pink travertine	100	23.67	−25.80	
KHM 18	−35	Pink marble-cement		18.68	−14.60	
KHM 19	−60	Pink marble-cement		23.68	−17.21	
KHM 21	−60	White marble-cement		18.37	−13.53	

Metre mark is the downward distance (in m) beneath the contact with the cement-marble unit. The content in calcite was determined by calcimetry or using the CO_2 yield provided by acid digestion for the purpose of isotopic analysis. C isotopic analysis of kerogen were done in Rennes and in CRPG Nancy (*).

4.2.4. Stalactites after concrete structures

Table 2 and Fig. 5 show that "rural" stalactites do not differ significantly by their C and O isotopic compositions from stalactites and carbonate coatings sampled on concrete structures in urban areas where the contribution of combustion CO_2 is poten-

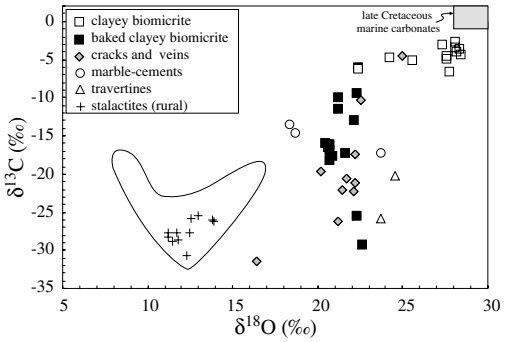

Fig. 5. $\delta^{13}C$ vs. $\delta^{18}O$ diagram for the Khushaym Matruk carbonate (carbonate fraction of the matrix in clayey biomicrites, newly-formed carbonates in cracks and travertines). The isotopic compositions of carbonate concretions (flowstones, stalactites) formed after concrete structures (envelope after data from McLeod et al., 1991; Krishnamurthy et al., 2003) and additional data from rural areas (crosses, this study) are also reported.

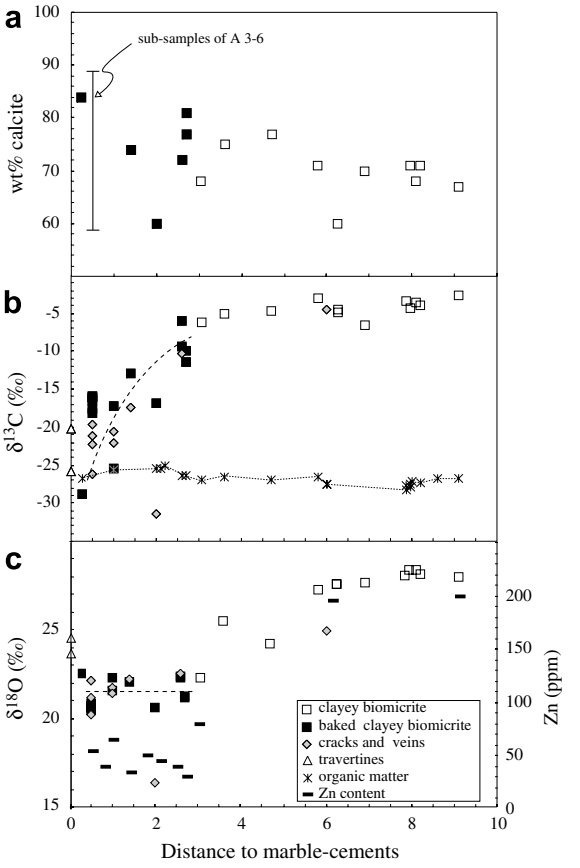

Fig. 6. Evolution of several parameters as a function of the distance to the contact (dashed line) with the cement-marble unit. (a) Calcite contents of the matrix in the clayey limestones. (b) $\delta^{13}C$ of carbonate fractions and organic matter in the matrix. (c) Variations of the bulk-rock Zn content and $\delta^{18}O$ of the carbonate fraction.

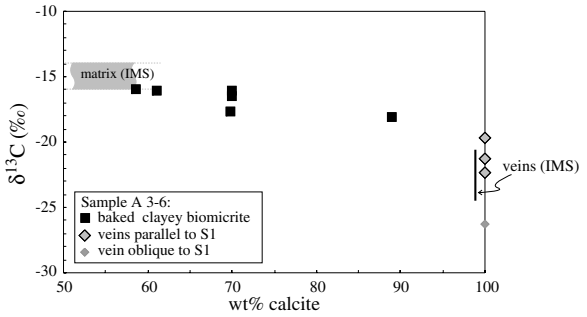

Fig. 7. Evolution of the C isotopic composition with the carbonate content in matrix sub-samples of baked biomicrite A3-6 (metre mark 0.5 m, see Fig. 2). See text for explanations.

tially non-negligible (e.g., McLeod et al., 1991; Krishnamurthy et al., 2003). Very significant in this respect is the fact that the most extreme $\delta^{13}C$-values measured in urban areas (*ca.* −30‰) are matched in rural areas.

4.3. Porosimetry measurements

At the hillfoot, clayey limestones are characterized by very high porosity values of 47.6% and 49.3% and average pore diameters of 0.12 and 0.14 μm (Table 3). Along the studied trench, both the porosity and the mean pore diameter decrease upward. The porosity decrease is thus concurrent with the lowering of bulk carbonate $\delta^{13}C$-values (Fig. 8). Among the studied samples, the minimum values are measured in level A3, i.e., in baked biomicrite KHM13 (15.6% and 0.016 μm).

4.4. Zn contents

A profile of the total concentration of Zn in bulk samples of biomicrite is shown in Fig. 6c. Total concentrations of Zn are lowest in the region close to the contact (about 50 ppm at distances less than 3 m from the contact) and increase to about a maximum of 200 ppm at 6 m away from the contact.

5. Discussion

5.1. pH of alkaline solutions

The presence of spurrite in the cement sets the temperature range at the time of combustion at about 1000–1100 °C (Bentor et al., 1972; Kolodny, 1979). Observation of the cement-marbles indicates the later alteration of spurrite as the process

Table 2
C and O isotopic compositions of some stalactites and flowstones formed after concrete structures in rural areas (France; numbers in brackets refer to the related department)

Echantillon	Locality	Type	$\delta^{18}O$	$\delta^{13}C$
Ti Clecy 1	Clecy (60)	Flowstone (railway bridge over Orne river)	13.86	−26.29
Boël 1	10 km South of Rennes (35)	Stalactite (railway bridge over Vilaine river)	11.82	−28.56
Boël 1 (external)	10 km South of Rennes (35)	Stalactite (railway bridge over Vilaine river)	12.50	−27.63
Boël 1 (internal)	10 km South of Rennes (35)	Stalactite (railway bridge over Vilaine river)	11.18	−28.24
Boël 2	20 km South of Rennes (35)	Stalactite (railway bridge over Vilaine river)	11.48	−28.78
Boux 1	11 km South of Rennes (35)	Stalactite (railway bridge over Vilaine river)	11.72	−27.73
Boux 2	12 km South of Rennes (35)	Stalactite (railway bridge over Vilaine river)	12.99	−25.45
Cabo 04-39	Beaulieu Campus, Rennes (35)	Stalactite (pedestrian concrete arch)	11.19	−27.77
Minou 04-41	Cape Minou, 10 km West of Brest (29)	Flowstone (concrete arch close to sea)	12.33	−30.77
Liz	Lizio (56)	Flowstone (below St Lubin fontain roof)	13.78	−25.95
Champ	Folies Siffait, 25 km East of Nantes (44)	Stalactite (concrete arch close to Loire river)	12.54	−25.83

Table 3
Porosity parameters obtained by Hg injection on a few representative samples of the Khushaym Matruk profile

Sample	Metre mark	Type	Porosity (%)	Mean pore diameter (μm)
A 1-1	9.1	Clayey biomicrite	49.27	0.135
A 2-2	8.1	Clayey biomicrite	47.60	0.123
A 3-1	2.7	Baked clayey biomicrite	21.91	0.047
A 3-4	1.4	Baked clayey biomicrite	20.82	0.023
KHM 13	2.0	Baked clayey biomicrite	15.63	0.015

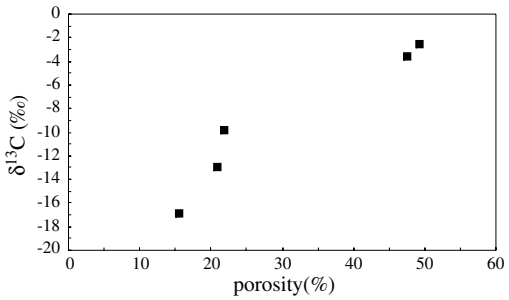

Fig. 8. Evolution of the C isotopic composition with the connected porosity for a few representative samples of biomicrites.

responsible for the genesis of high-pH solutions. The presence of the secondary minerals calcite–jennite–afwillite–brucite and of CSH phases in the fractures and altered matrix of the cement-marbles demonstrates the past circulation of high-pH solutions in the cement mass above the biomicrite layers. Thermodynamic equilibrium computations were performed using the code Chess 3.1 (Van der Lee and De Windt, 2000) in order to estimate the pH and temperature of the solutions and the potential equilibria between observed secondary minerals. Equilibrium constants for aqueous reactions and calcite were taken from the chess.2.5r3 database derived from the EQ3/6v8r6 (Lawrence Livermore National Laboratory) database. Thermodynamic data for jennite (Ca/Si = 1.5) was estimated using the solid solution model presented by Kulik and Kertsen (2001). Contradictory values are found for the afwillite equilibrium constant. Equilibrium constants derived from Kulik and Kertsen (2001) are in agreement with data found in the EQ3/6 database. Dickson et al. (2004) and the last version of the HATCHES database (Heath and Ilett, 2004; Bond et al., 1997) recently proposed significantly higher values for the formation constant of afwillite (e.g. −46.5 instead of −60.1 at 25 °C).

With the assumption of a temperature of 25 °C, a pH (25 °C) =12.0 is computed for a solution in equilibrium with calcite, jennite and tobermorite-14A (chosen to represent CSH phases). An assemblage between calcite, tobermorite and afwillite at 25 °C is possible when using the data of Dickson et al. (2004) and yields a pH of 11.1. An assemblage of calcite and tobermorite produces an equilibrium pH of 10.56 at 25 °C. When heated, such an assemblage becomes in equilibrium with afwillite (log$K$ of Dickson et al., 2004) at 46 °C and the pH of the solution is 10.06. Conditions corresponding to a state of close equilibrium between calcite, jennite, afwillite and tobermorite cannot be computed in a

system where water activity is fixed at 1. Portlandite was not observed among secondary phases, although precipitation of CSH gels upon spurrite alteration should leave an excess of Ca. The release of that Ca is expected to progressively induce oversaturation of the solution with respect to portlandite. The absence of portlandite suggests that carbonation of secondary products was possible during or after the alteration. The spatial distribution of mineral phases shows well crystallized afwillite and jennite in, or adjacent to, the fracture fillings instead of amorphous Ca–Si gels deeper inside the rock matrix bordering the fracture (see Section 4.1). This suggests a situation of a temperature gradient where temperatures are higher in the circulating fluid than in the bordering rock matrix. It is supported by phase diagrams presented in Atkinson et al. (1995) which show the stability of the jennite–afwillite association in the temperature range 80–120 °C, whereas CSH phases are more stable below 80 °C. This feature is consistent with a scenario in which hot waters are set in motion around the combustion front and alter cooling down cement-marble zones at some distance. Although, it is not possible to resolve completely the conditions that led to the coeval formation of the minerals identified in the fractures, possibly because factors like the amount of available water also controlled the afwillite–jennite equilibrium, thermodynamic calculations and mineralogical data suggest that high pH waters were generated at temperatures in the range 40–100 °C. The most probable pH range for these waters is from 10.5 to 12. Higher pH at lower temperature are not ruled out for closed subsystems in which the CO_2 control was less marked. The observation of zeolites and the absence of CSH phases in the upper levels of the sedimentary pile (Rassineux et al., 2001) is consistent with water-rocks interaction at pH around 11.5. Taking into account alteration patterns of the cement-marble (see Section 4.1), K^+ and SO_4^{2-} ions are expected to represent significant dissolved components in these high pH-waters. Such a feature is also encountered in the Western Springs at Maqarin (Alexander and Smellie, 1998), where modern alkaline waters were sampled. However, the precise composition of alkaline waters produced in Khushaym Matruk cannot be easily derived and compared to modern groundwater at Maqarin. Modern low-temperature alkaline waters in Maqarin have pH (25 °C) in the range 12.3–12.8. No direct evidence exists in Khushaym Matruk that support the presence of solutions with pH (25 °C) higher than 12 in the past. This could be due to different flow regimes and CO_2 access in these two sites.

In summary, observation of the altered marble-cements overlying the biomicrite illustrates the process of spurrite alteration and confirms the past circulation of high pH waters in the fracture network of the metamorphosed rocks. Thermodynamic calculations support a scenario in which spurrite alteration generated solutions with a maximum pH (25 °C) of ~12 (equilibrium with calcite, jennite and CSH).

5.2. Isotopic variations

In contrast to cement-marbles, the KHM baked biomicrites did not experience decarbonation from the lack of metamorphic minerals and the thermal profiles proposed by Elie et al. (2007). Consequently, recarbonation cannot be invoked in these rocks. The question to answer is whether the isotopic variations observed in baked biomicrites are due (i) to processes related to the combustion event or (ii) to the interaction of the rocks with alkaline solutions or (iii) to other diagenetic processes. In order to discuss these processes (Sections 5.2.3–5.2.6) the information relevant to the interpretation of isotopic ratios that come from independent tracers (Section 5.2.1) and from the Maqarin site (Section 5.2.2) must be stressed.

5.2.1. Assessment of basic constraints

(i) The sediments have undergone a strong isotopic (O,C) disturbance in relation with to proximity with the overlying cement-marbles (Fig. 6b).

(ii) *Net carbonation* occurred in macrofractures and within the matrix of upper biomicrites as microfractures and foraminifera tests infillings. The matrix carbonation is shown by cathodoluminescence observations: a newly-formed carbonate with luminescence properties similar to those of veins, fills increasing proportions of microcavities and foraminifera tests towards the contact with cement-marbles (Techer et al., 2006). The carbonation is also shown by the global increase of the carbonate content observed towards the cement-marbles (Fig. 6a) and this increase cannot be explained by a loss of organic matter upon heating, only.

(iii) Small-scale study of sample A3-6 argues that the δ^{13}C-values of baked biomicrites are explainable in terms of a *two-component mixture* involving a newly-formed carbonate component with very negative δ^{13}C-values and a less ^{12}C-enriched carbonate component. This is suggested by the "mixing" relationships of Fig. 7 and the "in situ" analysis of sample A3-6 (Fig. 3c). The less ^{12}C-enriched carbonate component ($\delta^{13}C \geqslant -14.9‰$, Fig. 3c), not entirely singled out by in situ analysis because the ion beam (30 μm) likely exceeds the grain size of the mixture, may correspond to an inherited, likely marine, composition. The other carbonate component, with more negative δ^{13}C-values (e.g., foraminifera infillings), is close to the carbonate phase found in most macro- and micro-veins and represents newly-formed carbonate.

(iv) Fig. 8 shows that both porosity and δ^{13}C-values decrease towards the contact with the metamorphic unit. Consequently, carbonation reactions likely contributed to the porosity decrease in the baked biomicrites.

(v) With the exception of vein KHM13 that also has the lowest C isotopic signature: $\delta^{13}C = -31.4‰$, all the matrixes and veins above metre mark 3 have comparable O isotopic compositions. These O isotopic compositions correspond to isotopic equilibrium between calcite and local rainfall at near-surface temperature and in near-neutral pH conditions. Fig. 9 illustrates the equilibrium temperatures found using the isotopic fractionation coefficients of O'Neil et al. (1969) and taking into account possible variations of the rainfall compositions during the last 150 ka, a time period that encompasses glaciation events. This was done by slightly decreasing the mean δ^{18}O-value ($-6.5‰$) of the present-day rainfall given by Rozanski et al. (1993) in Amman (Jordan), down to $-8‰$, which appears reasonable considering the Mediterranean environment of Jordan. It is worth noting that present-day high-pH springs in Maqarin have temperatures of 24–26 °C (Alexander and Smellie, 1998, and references therein).

(vi) Sr isotopic ratios argue that the Ca involved in the newly-formed carbonate from veins was derived from the cement-marble metamorphic unit (Techer et al., 2006).

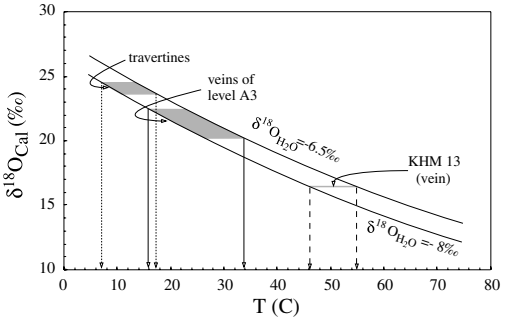

Fig. 9. Diagram depicting the formation temperature ("*x*"-axis) as a function of the O isotopic composition of the newly-formed carbonates ("*y*"-axis), using δ^{18}O-values in the range $-6.5‰$ to $-8‰$ for past rainfall in Jordan (see text for explanations).

(vii) Mineralogical markers (Rassineux, 2001; Rassineux et al., 2001; Techer et al., 2006) as well as the structure of organic matter in the sediments (Elie et al., 2007) argue for the input of hyperalkaline solutions mostly within the upper 3 m of sediment located beneath the metamorphic unit. The covariation of the Zn content and the δ^{18}O value in the 3-m zone near the contact (Fig. 6c) give further evidence for the circulation of high pH solutions in that layer. An important change in Zn speciation occurs between pH 11 and 12 (Baes and Maesmer, 1976). Above pH (25 °C) ~11.5, the aqueous speciation of Zn is dominated by the ZnO_2^{2-} oxyanion that cannot be incorporated in calcite like the Zn^{2+} ion at lower pH in supergene conditions (smithsonite or hydrozincite components; see Hitzman et al., 2003 for a recent review). Zinc solubility and mobility is thus predicted to increase strongly at pH >11.5 and this is consistent with the observed profile. Because carbonate also influences Zn solubility (hydrozincite, smithsonite), a spectroscopic study of Zn solid-state speciation (e.g. EXAFS) could, in a future investigation, help to bracket the pH-pCO_2 conditions that prevailed along the profile.

5.2.2. The Maqarin reference

In the Maqarin site which is also located in Jordan and is hydrologically active today, Clark et al. (1993) explained the low C and O isotopic compositions of the different carbonate types in cement-marbles as resulting from a sequence of events that involve: (i) isotopic fractionation during decarbon-

ation, (ii) hydration/recarbonation involving H_2O vapour and a combustion CO_2 derived from both oxidization of organic matter and from decarbonation. Such a CO_2 will be hereafter named "combustion" CO_2. Considering the similarity of the C and O isotopic compositions of cement-marbles in the sites of KHM and Maqarin as well as the common size of the combustion units and the similar peak temperatures, the explanation advocated by Clark et al. (1993) in Maqarin likely works for the Khushaym Matruk cement-marbles, even though the sediments here are somewhat richer in the clay component than those of Maqarin.

5.2.3. High temperature isotopic exchange related to the combustion event

$\delta^{13}C$ variations could be seen as resulting from thermally-induced isotopic exchange between the carbonate component and (i) the organic matter contained in the sediment and/or (ii) the CO_2 gas released from adjacent combustion zones. High-temperature isotopic exchange between organic matter and the carbonate fraction would lead the C isotopic compositions to converge. The rather constant $\delta^{13}C$-value of organic matter (Table 1, Fig. 6b) is at variance with this hypothesis, except in the highly unrealistic case where the C rock fraction contained in the organic matter would have been an infinite isotopic reservoir during exchange.

Equilibration with CO_2 gas also fails to explain the data. According to Clark et al. (1993) and using the calcite-CO_2 equilibrium fractionation coefficients of Bottinga (1968) or Zheng (1994), the $\delta^{13}C$-value of CO_2 released from the combustion unit should be in the interval $-26‰$ (burned organic matter) and slightly positive values (decarbonation CO_2, typically *ca.* $+3‰$/PDB). The $\delta^{18}O$-value of this CO_2 should range between *ca.* +25 and +35/37‰/SMOW (combined atmospheric O_2 and decarbonation CO_2, respectively). So, a lowering of carbonates $\delta^{13}C$-values down to the range observed in the profile is theoretically possible as depicted in Fig. 10. Nevertheless, this scenario is hardly compatible with the fact that the C isotopic composition of the organic matter is not significantly affected in the hottest part of the profile, i.e. the A3 level. Secondly, the increase of the carbonate content towards the cement-marbles (Fig. 6a) is not explained by a process of isotopic exchange. Neither the difference in Sr isotopic ratios between carbonate from veins and from biomicrites nor the rather constant $\delta^{18}O$-values of carbonate in the baked biomicrites

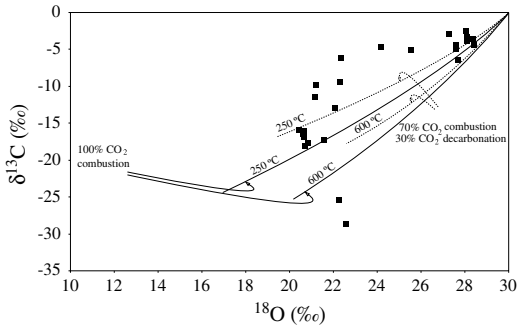

Fig. 10. Evolution of the C and O isotopic compositions of calcite during CO_2/rock isotopic equilibration under variable gas/rock ratio (CO_2 considered as an infinite O isotopic reservoir in the case of a mixed CO_2–H_2O gas). The curves represent the isotopic trajectories calculated for a maximum temperature of 600 °C (no presence of metamorphic minerals in the rock) and at 250 °C, a reasonable minimum peak temperature reached at 1 m away from the cement-marble, according to Elie et al., 2007. Pure combustion CO_2 and mixed combustion CO_2 were tested (see text for explanations).

(Fig. 10) are explained in such a context. The involvement of H_2O steam in the gas system (dehydration of clays and organic matter during combustion and/or input of heated meteoric water) as advocated in the Maqarin cement-marbles (Clark et al., 1993), introduces an additional difficulty. The O isotopic composition of the gas phase is unpredictable in that case because it varies with the origin of water, the degree of water evaporation/condensation, the gas CO_2/H_2O mass ratio and the degree of isotopic equilibration between gas and recharge or discharge host lithologies. Taking into account the sharp temperature gradient that existed in the baked biomicrites during the thermal peak (Elie et al., 2007), the rather constant $\delta^{18}O$-values in this zone are not easily explained (Table 2, Fig. 6b). From the above arguments, it remains that gas/rock isotopic exchange does not appear to be the major process that produced the isotopic variations in the KHM baked biomicrites. The isotopic variations cannot be disconnected from the carbonation processes observed in these sediments.

5.2.4. Carbonation related to high-pH solutions

^{12}C-enriched carbonate is common in the context of hyperalkaline solutions. Because the presence of such solutions is established in KHM, it is tempting to relate the measured low $\delta^{13}C$ to their input. Numerous papers have been devoted to these carbonation processes in the past, most of them

dealing with concretions after weathered concrete structures (e.g., McLeod et al., 1991; Létolle et al., 1992; Dietzel et al., 1992; Krishnamurthy et al., 2003) but also to carbonation driven by alkaline solutions coming from the weathering of ultramafic rocks (O'Neil and Barnes, 1971; Clark et al., 1992). Usdowski and Hoefs (1986), Létolle et al. (1990a,b), Dietzel et al. (1992) and Clark et al. (1992) discussed the different kinetic mechanisms by which both enrichments in ^{12}C and ^{16}O could occur during CO_2 gas uptake by hyperalkaline solutions. The maximum δ ^{13}C depletions, in the range $-17‰$ to $-19‰$, are explained for experiments on $Ba(OH)_2$ or $Ca(OH)_2$solutions (Usdowski and Hoefs, 1986; Dietzel et al., 1992; Clark et al., 1992) and may induce carbonate $\delta^{13}C$-values down to *ca.* $-26‰$, starting with a "modern" atmospheric CO_2 at $-8‰$. A contribution of "organic-matter-derived C" (e.g. in Maqarin related to the combustion of organic matter, Clark et al., 1993) or additional isotopic fractionations (see discussion and references in Krishnamurthy et al., 2003) was invoked to explain some carbonates with still lower isotopic compositions (down to *ca.* $-30‰$). The isotopic measurements on rural stalactites formed after weathered concrete structures (Table 3) demonstrate that the production of concretions with extreme ^{13}C-depletions does not require the contamination of the local atmosphere by combustion or respiration CO_2.

In the KHM site, vein sample KHM13 (Table 1, Fig. 2) illustrates the uptake of CO_2 gas by hyperalkaline solutions with kinetic effects for C ($\delta^{13}C = -31.4‰$). The O isotopic composition ($\delta^{18}O = +16.4‰$) is lower than the value expected for equilibrium with local groundwater in superficial temperature conditions. However, it does not necessarily imply kinetic O fractionation. Recent work has shown the strong dependence of the $^{18}O/^{16}O$ ratio of dissolved inorganic C (DIC) with pH (Cory-Beck et al., 2005). According to this work, the O isotopic composition of vein KHM13 is close to what is predicted for equilibrium with local groundwater at pH >10. The low $\delta^{13}C$-values of travertines ($-20.1‰$ to $-28.7‰$) are also compatible with formation from high pH solutions. All the other newly-formed carbonates display similarly low C isotopic ratios including those filling up microcracks and foraminifera tests. Uptake of atmospheric CO_2 was invoked for such low $\delta^{13}C$ travertines found in the vicinity of other Jordanian cement-marbles formed in ancient lakes of alkaline water or in areas where alkaline solutions are presently seeping away (Clark et al., 1991). The location of most KHM travertines at the bottom of the metamorphic unit where a number of cavities are observed is compatible with the existence of a high permeability level here, both for air and for alkaline solutions. The same non-saturated conditions may also hold for the thick vein KHM13, which has a laminar structure indicating a recurrent fracture opening (Techer et al., 2006). Large air/liquid ratios may still be admitted if the sweating alkaline solution formed a film coating the walls of an open fracture. However, kinetic effects cannot be considered in the other veins and overall, in the microporosity (Fig. 3c). Access of atmospheric CO_2 to this microporosity might have been very limited. Moreover, the CO_2 uptake in such a situation would have been likely quantitative (see experiments of Clark et al., 1992), resulting in a lack of C isotopic fractionation. In these objects, the $\delta^{13}C$-value of newly-formed carbonate should mimic that of DIC in the solution and so, the involvement of "combustion CO_2" is an alternative explanation. This suggests that "combustion CO_2" introduced and stored in the sediments reacted with the Ca^{2+}-bearing alkaline solutions coming from cement-marbles to produce carbonate, when rehydration of the system occurred. In such a context, an alternative explanation for the $^{87}Sr/^{86}Sr$ composition measured (Techer et al., 2006) in carbonate veins may be a remobilisation of the Sr from the fracture wall-rocks attacked by alkaline fluids. Indeed, it is likely that some radiogenic Sr is released into the solution during clay transformation (beidelleite → montmorillonite), but the process cannot be quantified in the light of available data on the Sr isotopic ratio of secondary clays. However, the low $\delta^{18}O$ expected for newly-formed carbonate formed with high pH solutions (kinetic or equilibrium fractionations) are lacking, except in vein KHM13. Therefore, for most of the carbonation material, additional processes or different carbonation conditions have to be discussed.

5.2.5. Putative role of hot alkaline solutions

The isotopic behaviour of carbonation systems involving hot alkaline solutions is poorly known. Although some kinetic C and O isotopic effects related to CO_2 uptake and hydroxylation are expected, isotopic re-equilibration would likely alter these C and O isotopic signatures after carbonate crystallization (and the decrease of pH) because the kinetics of isotopic exchange in the $CaCO_3$–

$H_2O(CO_2)$ system increase with temperature. Therefore, the isotopic compositions of the KHM baked biomicrites may reflect carbonation with hot alkaline solutions followed by "hot" isotopic reequilibration. Given the fact that the O isotopic composition of liquid H_2O (condensed steam?) and "combustion" CO_2 are not constrained in KHM, we have no positive arguments to demonstrate this mechanism but it is not at variance with the other data available in KHM. Basically, it would be an extension of the alteration processes advocated by Clark et al. (1993) in the Maqarin cement-marbles and would have quickly followed the combustion event. Nevertheless, two points are intriguing in such a scenario. First, the fact that the present-day O isotopic composition of all the carbonate fractions in the baked biomicrites (except vein KHM13) is close to the equilibrium value with local groundwater at superficial temperatures may be seen as an noticeable coincidence in the "hot" carbonation scenario. Secondly, the Maqarin site which is hydrologically active today, differs from the hydrologically dead KHM site, by the presence of apparent equilibrium O isotopic values in the latter while δ^{13}C-values are comparable (see Clark et al., 1993). This strongly suggests low-temperature equilibration and some ageing isotopic effect.

5.2.6. Post-carbonation isotopic re-equilibration with "cold" groundwater

Post-formation isotopic re-equilibration with continental hydrosphere is common in carbonate sediments when they recrystallize (e.g., Dickson and Coleman, 1980), for example in relation to variations of the water table (e.g., Magaritz, 1974). The process is enhanced if calcite is produced by inversion of its polymorphs. In high-pH carbonation systems, either natural (e.g., Kolodny and Gross, 1974; Khoury and Nassir, 1982; Clark et al., 1993) or experimental (e.g., Lanas and Alvarez, 2004), polymorphs of calcite are often produced (aragonite and/or vaterite). Isotopic reequilibration of both calcite and its polymorphs during recrystallization related to variations of the water table is a possible mechanism in Khushaym Matruk but it requires a more or less selective isotopic re-equilibration of O (Fig. 4). Generally, both O and C isotopic systems are affected (see O'Neil, 1987, and references therein) but if negligible amounts of externally-derived C are introduced into the system, only δ^{18}O would be modified. From the comparison of fossil and modern carbonate crusts considered to be formed from alkaline solutions in Oman, Clark et al. (1992) suggested that fossil carbonate experienced a large degree of post-formation isotopic reequilibration in superficial conditions with up to a 10 δ-units increase both for C and O. If present in KHM, such effects imply that O reached secondary isotopic equilibrium and that the C isotopic signatures of pristine newly-formed carbonates were possibly lighter than presently measured. Vein KHM13 could be seen as a partially reequilibrated system, half-way between the signatures of common concretions formed in the context of alkaline solutions and the equilibrium values. If true, the re-equilibration hypothesis suggests that the carbonates formed with – or submitted to – alkaline solutions are "isotopically metastable" and are more susceptible to O isotopic exchange than common calcite.

5.3. Depth propagation of the alkaline front

Mineralogical markers (Rassineux, 2001; Rassineux et al., 2001) and geochemical tracers (Zn contents, isotopic compositions, structure of organic matter) observed in the bottom of the profile (A2 and A1 levels) suggest that the impact of alkaline solutions quickly vanishes downwards. Carbonation of the matrix porosity still exists below level A3. This is supported by the presence of carbonate infillings in foraminifera (e.g., very abundant in sample A2-10 at metre-mark 4.7) but the proportion of such newly-formed cements quickly decreases downwards (Rassineux, 2001). Therefore, it is not possible to give a precise limit to the propagation of high-pH solutions since subtle effects on the C isotopic composition may locally be present at *ca.* 7 m from the contact (sample A2-7, Table 1). Several factors controlled the spatial imprint of alkaline solutions. The buffering capacity of the clay component in biomicrite and that of the CO_2 uptake during fluid migration progressively decreased the pH of the solution. Indeed, below the A3 level, detrital quartz and feldspar are not totally dissolved, the transformation beidellite/montmorillonite is not complete, which indicates that the time-integrated buffering front is situated beneath indurate level A3. Carbonation reactions reduced the porosity in the baked biomicrites with a likely concomitant decrease of permeability and this has most probably limited the further migration of alkaline solutions across the section. Thus, the major consequence of the migration of alkaline solution is sealing off.

The major climatic changes that are suspected during the Pleistocene with arid conditions following a humid climate (Clark et al., 1991) might have also been an important factor for the site evolution. During the recent period, episodic and meagre rainfall events may have been insufficient for providing significant amounts of alkaline solutions into the sediments and the level of the water table was likely far below the interface with the metamorphic unit. The present day location of the "alkaline front" would not reflect, in that case, an intrinsic property of the sedimentary medium, namely its sealed character, but rather the cessation in the front progression due to a decline in the supply of alkaline solutions. The poor knowledge of the past climatic evolution and of the hydrological behaviour in the Kushaym Matruk area, especially the pathway of alkaline solutions, precludes a straightforward answer to that question.

6. Concluding remarks

In the Khushaym Matruk sediments, the O and C isotope variations occur mostly within the upper 3 m of sediments, which coincides with the zone where the mineralogical and chemical markers sensitive to the input of high pH solutions are the most modified. The isotopic variations are likely witnesses of the interaction between sediments and such alkaline solutions, especially via a well-defined carbonation process. Some uncertainties remain in the interpretation of isotopic characteristics. The most puzzling feature in these rocks is the lack of O isotopic disequilibrium with respect to local groundwater, such disequilibria being common during the production of carbonate from highly alkaline solutions. This suggests some post-formation re-equilibration of the carbonate fraction, which affected the O rather than the C signature. Carbon addition from a "combustion CO_2" and locally from the atmosphere are likely but the temperature of the carbonation process is not constrained.

It is questionable to compare the Khushaym Matruk site with an industrial concrete/clayey repository medium. First, although alkaline, the solutions released from the KHM cement-marbles had a pH value $\leqslant 12$, which is lower than the value of solutions released from a fresh concrete ($pH = 13.3$) or from a "used" concrete that had lost its alkali-elements: $pH = 12.5$. Secondly, a significant difference is the fact that, in KHM, a major buffering agent of the alkaline solutions was CO_2, whatever its origin (combustion- and atmosphere-derived), in addition to the silicate phases. This aspect does not totally disconnect the studied site from repository settings. Indeed, in several countries, the forecast repository media are clay-rich formations weakly affected by diagenesis. Such rocks contain organic matter among other components, and it was recently recognized that CO_2 was one non-negligible component of the pore fluid. This CO_2 may be produced from the very early transformation stages of organic matter, at low temperatures (Deniau et al., 2005; Wersin et al., 2005) and from fluid equilibration with the host rocks carbonate component (Girard et al., 2005). For that reason, the Khushaym Matruk behaviour might have some relevance to the initial lifetime stages of a repository site during which re-saturation and gas circulation are expected to occur.

Acknowledgements

This study is part of the Maqarin Phase IV Project that was supported by Andra, CEA, JNC, Nagra, Nirex, SKB and the University of Jordan (Prof. H. Khoury). The Centre National de la Recherche Scientifique (CNRS) and Agence Nationale pour la Gestion des Déchets Radioactifs (ANDRA) are thanked for providing the financial support for this research *via* the GdR FORPRO (action FORPRO 2001.VII). W.R. Alexander (RWIG, University of Bern, Switzerland) and E. Jacquot (ANDRA) are acknowledged for helpful discussions as well as J. Cornichet for help during the isotope analytical session. Thanks are due to I.D. Clark and to an anonymous reviewer for reviewing an earlier version. The paper greatly benefited from constructive suggestions by I.D. Clark. This is the GDR FORPRO contribution number (2005)7A.

References

Adenot, F., Buil, M., 1992. Modelling of the corrosion of cement paste by de-ionized water. Cem. Concr. Res. 22, 489–496.

Adler, M., Mäder, U., Waber, N., 1999. High-pH alteration of argillaceous rock: an experimental study. Schweiz. Mineral. Petrog. Mitt. 79, 445–454.

Alexander, W.R., Smellie, J.A.T., 1998. Maqarin natural analogue project: ANDRA, CEA, NAGRA, NIREX and SKB synthesis report on phases I, II and III. Scientific Technical Report NPB 98-08.

Alexander, W.R., Dayal, R., Eagleson, K., Eikenberg, J., Hamilton, E., 1992. A natural analogue of high pH cement pore waters from the Maqarin area of northern Jordan. II: results of predictive geochemical calculations. J. Geochem. Explor. 46, 133–146.

Atkinson, A., Harris, A.W., Hearne, J.A., 1995. Hydrothermal alteration and ageing of synthetic calcium silicate hydrate gels. Safety Series Reports NSS/R374, UK Nirex Limited, Harwell, UK.

Baes, C.F., Maesmer, R.E., 1976. The Hydrolysis of Cations. Wiley, New York.

Bateman, K., Combs, P., Noy, D.J., Pearce, J.M., Wetton, P., Haworth, A., Linklater, C., 1999. Experimental simulation of the alkaline disturbed zone around a cementitious radioactive waste repository: numerical modelling and column experiments. In: Metcalfe, R., Rochelle, C.A. (Eds.), Chemical Containment of Waste in the Geosphere, vol. 157. Geol. Soc. London Spec. Publ., pp. 183–194.

Bauer, A., Berger, G., 1998. Kaolinite and smectite dissolution rate in high molar KOH solutions at 35 °C and 80 °C. Appl. Geochem. 13, 905–916.

Bauer, A., Velde, B., 1999. Smectite transformation in high molar KOH solutions. Clay Min. 34, 259–273.

Bentor, Y.K., Gross, S., Kolodny, Y., 1972. New evidence of the origin of the high temperature mineral assemblage of the "Mottled Zone" (Israel). In: Proceeding of the 24th International Geol. Cong., Montréal.

Bond, K.A., Heath, T.G., Tweed, C.J., 1997. HATCHES: a referenced thermodynamic database for chemical equilibrium studies. Nirex Report NSS/R379, December 1997.

Bottinga, Y., 1968. Calculation of fractionation factors for carbon and oxygen isotopic exchange in the system calcite-carbon dioxide-water. J. Phys. Chem. 72, 800–808.

Braney, M.C., Haworth, A., Jefferies, N.L., Smith, A.C., 1993. A study of the effects of an alkaline plume from a cementitious repository on geological materials. J. Contam. Hydrol. 13, 379–402.

Clark, I.D., Khouri, H.N., Salameh, E., Fritz, P., Göksu, Y., Wieser, A., Causse, C., Fontes, J.C., 1991. Travertines in central Jordan. Implications for paleohydrology and dating. In: Proceeding of the IAEA Symposium 312, Use of Isotope Techniques in Water Resource Development, March 11–15, 1991, pp. 551–565.

Clark, I.D., Fontes, J.-C., Fritz, P., 1992. Stable isotope disequilibria in travertine from high pH waters: laboratory investigations and field observations from Oman. Geochim. Cosmochim. Acta 56, 2041–2050.

Clark, I.D., Fritz, P., Seidlitz, H.K., Trimborn, P., Milodowski, T.E., Pearce, J., 1993. Recarbonation of metamorphosed marls, Jordan. Appl. Geochem. 8, 473–481.

Cory Beck, W., Grossman, E.L., Morse, J.W., 2005. Experimental studies of oxygen isotope fractionation in the carbonic acid system at 15°, 25°, and 40 °C. Geochim. Cosmochim. Acta 69, 3493–3503.

Deniau, I., Béhar, F., Largeau, C., De Cannière, P., Van Geet, M., Beaucaire, C., Pitsch, H., 2005. Early CO_2 and polar liquid production from the Boom Clay kerogen upon thermal stress in relation with waste disposal. In: ANDRA Internat. Meeting, Tours (France), March 14–18th, 2005, Clays in natural and engineered barriers for radioactive waste confinement". Abstr. vol. O/07B/4, pp. 117–118.

De Windt, L., Pellegrini, D., Van Der Lee, J., 2004. Coupled modelling of cement/claystone interactions and radionuclide migration. J. Contam. Hydrol. 68, 165–182.

Dickson, J.A.D., Coleman, M.L., 1980. Changes in the carbon and oxygen isotopic composition during limestone diagenesis. Sedimentology 27, 107–118.

Dickson, C.L., Brew, D.R.M., Glasser, F.P., 2004. Solubilities of CaO-SiO_2-H_2O phases at 25 °C, 55 °C and 85 °C. Adv. Cement Res. 16, 35–43.

Dietzel, M., Usdowski, E., Hoefs, J., 1992. Chemical and $^{13}C/^{12}C$- and $^{18}O/^{16}O$-isotope evolution of alkaline drainage waters and the precipitation of calcite. Appl. Geochem. 7, 177–184.

Eberl, D.D., Velde, B., McCormick, T., 1993. Synthesis of illite-smectite from smectite at earth surface temperatures and high-pH. Clay Miner. 28, 49–60.

Elie, M., Techer, I., Trotignon, L., Khoury, H., Salameh, E., Vandamme, D., Boulvais, P., Fourcade, S., 2007. Cementation of kerogen-rich marls by alkaline fluids released during weathering of thermally metamorphosed marly sediments. Part II: Organic matter evolution, magnetic susceptibility and metals (Ti, Cr, Fe) at the Khushaym Matruk natural analogue (Central Jordan). Appl. Geochem. 22, 1311–1328.

Gaucher, E.C., Blanc, P., Matray, J.-M., Michau, N., 2004. Modeling diffusion of an alkaline plume in a clay barrier. Appl. Geochem. 19, 1505–1515.

Girard, J.P., Fléhoc, C., Gaucher, E., Buschaert, S., 2005, Stable isotope composition of porewater in Callovian-Oxfordian argillites (Bure): insight from CO_2 and H_2O-vapor released by cores. In: ANDRA Internat. Meeting, Tours (France), March 14–18th, 2005. "Clays in Natural and Engineered Barriers for Radioactive Waste Confinement", Abstr. Vol., O/15A/4, pp. 239–240.

Heath, T.G., Ilett, D.J., 2004. HATCHES, the Harwell/Nirex Thermodynamic Database for Chemical Equilibrium Studies. Serco Assurance, Harwell International Business Centre, Oxfordshire, UK.

Herbert, H.J., Kasbohm, J., Henning, K.H., 2002. Long term behaviour of the Wyoming bentonite MX-80 in high alkaline solutions. In: ANDRA International Meeting, Clays in Natural and Engineered Barriers for Radioactive Waste Confinement, December 9–12, 2002, Reims, France.

Hitzman, M.W., Reynolds, N.A., Sangster, D.F., Allen, C.R., Carman, C.E., 2003. Classification, genesis and exploration guides for nonsulfide zinc deposits. Econ. Geol. 98, 685–714.

Khoury, H., Nassir, S., 1982. High temperature mineralization in Maqarin area, North Jordan. Neues Jahrb. Miner. Abh. 144, 197–213.

Khoury, H., Salameh, E., Abdul-Jaber, Q., 1985. Characteristics of an unusual highly alkaline water from the Maqarin area, Northern Jordan. J. Hydrol. 81, 79–91.

Khoury, H., Salameh, E., Clark, I.D., Fritz, P., Bajjali, W., 1992. A natural analogue of high pH cement pore waters from the Maqarin area of northern Jordan. I: introduction to the site. J. Geochem. Explor. 46 (1), 117–132.

Kolodny, Y., 1979. Natural cement factory: a geological story. In: Skalny, J. (Ed.), Cement Production and Use, Eng. Foundation Conf., Rindge, NH, USA, 24–29 June, pp. 203–216.

Kolodny, Y., Gross, S., 1974. Thermal metamorphism by combustion of organic matter: isotopic and petrological evidence. J. Geol. 82, 489–506.

Krishnamurthy, R.V., Schmitt, D., Atekwana, E.A., Baskaran, M., 2003. Isotopic investigations of carbonate growth on concrete structures. Appl. Geochem. 16, 435–444.

Kulik, D.A., Kertsen, M., 2001. Aqueous solubility diagrams for cementitious waste stabilization systems: II. End member

stoichiometries of ideal calcium silicate hydrate solid solutions. J. Am. Ceram. Soc. 84, 3017–3026.

Lanas, J., Alvarez, J.I., 2004. Dolomitic limes: evolution of the slaking process under different conditions. Thermochim. Acta 423, 1–12.

Létolle, R., Gaveau, B., Gegout, P., Moranville-Regourd, M., 1990a. Isotope fractionation of the ^{18}O during precipitation of carbonates at very high pH. Compt. Rend. Acad. Sci. 311, 547–552.

Létolle, R., Gegout, P., Moranville-Regourd, M., 1990b. Isotope fractionation of carbon during precipitation of carbonates at very high pH. Compt. Rend. Acad. Sci. 311, 95–99.

Létolle, R., Gegout, P., Rafia, N., Revertegat, E., 1992. Stable isotopes of carbon and oxygen for the study of carbonation/decarbonation in concrete. Cement Concrete Res. 22, 235–240.

Magaritz, 1974. Lithification of chalky limestone: a case study in Senonian rocks from Israel. J. Sed. Petrol. 44, 947–954.

McCrea, J.M., 1950. On the isotope chemistry of carbonates and a paleotemperature scale. J. Chem. Phys. 18, 849–857.

McLeod, G., Fallick, A.E., Hall, A.J., 1991. The mechanism of carbonate growth on concrete structures, as elucidated by carbon and oxygen isotope analyses. Chem. Geol. (Isotope Geosci. Sect.) 86, 335–343.

Mosser-Rück, R., Cathelineau, M., 2004. Experimental transformation of Na,Ca-smectite under basic conditions at 150 °C. Appl. Clay Sci. 26, 259–273.

O'Neil, J.R., 1987. Preservation of H, C, and O isotopic ratios in the low temperature environment. In: Kyser, T.K. (Ed.), Stable Isotope Geochemistry of Low Temperature Fluids, vol. 13. Min. Assoc. Canada, pp. 85–128.

O'Neil, J.R., Barnes, I., 1971. ^{13}C and ^{18}O compositions in some fresh water carbonates associated with ultramafic rocks and serpentinites, Western United States. Geochim. Cosmochim. Acta 35, 687–697.

O'Neil, J.R., Clayton, R.N., Mayeda, T.K., 1969. Oxygen isotope fractionation in divalent metal carbonates. J. Chem. Phys. 51, 5547–5558.

Ramirez, S., Cuevas, J., Vigil, R., Lequey, S., 2002. Hydrothermal alteration of 'La Serrata' bentonite (Almeria, Spain) by alkaline solutions. Appl. Clay Sci. 21, 257–269.

Rassineux, F., 2001. Project Maqarin: Phase IV. Contribution à l'identification des transformations minéralogiques de la biomicrite au contact de solutions alcalines sur le site de Khushaym Matruk. Rapport Final. D RP 0ERM 01-019.

Rassineux, F., Griffault, L., Smellie, J., Trotignon, L., Raynal, J., Khoury, H., Mercier, F., 2001. Mineralogical evolution of clay-bearing rock during alkaline alteration (Khushaym Matruk, Central Jordan). In: Cidu, R. (Ed.), Proceeding of the 10th International Symposium Water Rock Interaction (WRI-10), Villasimius Italy, pp. 1363–1366.

Rollion-Bard, C., Chaussidon, M., France-Lanord, C., 2003. pH control on oxygen isotopic composition of symbiotic corals. Earth Planet. Sci. Lett. 215, 275–288.

Rozanski, K., Araguas-Araguas, L., Gonfiantini, R., 1993. Isotopic patterns in modern global precipitation. In: Climate change in continental records, Geophys. Monograph 78, A.G.U., pp. 1–36.

Savage, D., Noy, D., Mihara, M., 2002. Modelling the interaction of bentonite with hyperalkaline fluids. Appl. Geochem. 17, 207–223.

Smellie, J.A.T., 1998. Maqarin Natural Analogue Study Phase III/SKB Technical Report 98-04. Stockholm: SKB Swedish Nuclear Fuel and Waste Management Co.

Soler, J., 2003. Reactive transport modelling of the interaction between a high-pH plume and a fractured marl: the case of Wallenberg. Appl. Geochem. 18, 1555–1571.

Techer, I., Fourcade, S., Elie, M., Martinez, L., Boulvais, P., Claude, C., Clauer, N., Pagel, M., Hamelin, B., Lancelot, J., 2004. Contribution des analogues naturels à la compréhension du comportement à long terme des milieux argileux vis à vis de la circulation de fluides hyper-alcalins/ Etude du site de Khushaym Matruk en Jordanie Centrale; géochimie isotopique du Sr, du C et de l'O, datations U-Th, K-Ar, caractérisation de la matière organique. Rapport Scientifique final Action 2001.VII GdR ForPro, # ForPro 2004/01 Rf.

Techer, I., Khoury, H.N., Salameh, E., Rassineux, F., Claude, C., Clauer, N., Pagel, M., Lancelot, J., Hamelin, B., Jacquot, E., 2006. Propagation of high-alkaline fluids in an argillaceous formation: case study of the Khushaym Matruk natural analogue (Central Jordan). J. Geochem. Explor. 90, 53–67.

Usdowski, E., Hoefs, J., 1986. $^{13}C/^{12}C$ partitioning and kinetics of CO_2 absorption by hydroxide buffer solutions. Earth Planet. Sci. Lett. 80, 130–134.

Van der Lee, J., De Windt, L., 2000. Chess Tutorial and Cookbook. User's Manual, Technical Report LHM/RD/00/13, CIG, Ecole des Mines, Fontainebleau, France.

Wersin, P., De Cannière, P., Pearson, F.J., Gaucher, E., Höhener, P., Eichinger, L., Mettler, S., Mäder, U., Vinsot, A., Gäbler, H.-E., Hama, K., Hernan, P., 2005. Results from an in situ porewater chemistry experiment in Opalinus clay: evdence of microbially-mediated anaerobic redox processes. ANDRA Internat. Meeting, Tours (France), March 14–18th, 2005. "Clays in Natural and Engineered Barriers for Radioactive Waste Confinement", Abstr. Vol., O/07B/2, pp. 113–114.

Zheng, Y.F., 1994. Oxygen isotope fractionation in metal monoxides. Mineral. Mag. 58A, 1000–1001.